J Mater Sci (2009) 44:3043–3048
DOI 10.1007/s10853-009-3402-2

Density of states effective mass of $SnBi_4Se_7$ deduced from the temperature dependence of electrical conductivity in the activation regime

S. A. Ahmed · S. H. Mohamed

Received: 15 February 2008 / Accepted: 16 March 2009 / Published online: 7 April 2009
© Springer Science+Business Media, LLC 2009

Abstract Current–voltage (*I–V*) measurements on polycrystalline samples of Bi_2Se_3 and stoichiometric ternary compound in the quasi-binary system of $SnSe–Bi_2Se_3$ at different temperatures in the vicinity of room temperature have been performed. Also, temperature dependence of electrical conductivity has been measured. From the analysis of the temperature dependence of electron concentration in the activation regime above room temperature, the density of states effective mass, m^*, has been determined. Some intrinsic and contact properties such as barrier heights, ideality factors, and carriers concentrations have been investigated using *I–V* characteristics. It has been found that all samples exhibit ohmic and space charge limited conduction at low and high fields, respectively.

Introduction

Bi_2Se_3 and their solid solutions are nowadays applied in the construction of thermoelectric generators and coolers, operating in the temperature range around 300 K [1]. Therefore, studies of the effect of impurities on the physical properties of Bi_2Se_3 are interesting for basic and applied research.

In more recent years considerable attention has been focused on Bi_2Se_3 and their solid solutions. Structural, electrical, and optical properties are reported by a few investigators [2–9]. Navratil et al. [10] reported that the calculated value of density of state effective mass for Bi_2Se_3 is $m^* = 0.15m_e$. On the other hand, according to Nikam et al. [11], films of Bi_xSe_{1-x}, where x is greater than 0.6, exhibit ohmic conduction and those with x varying between 0 and 0.6 show nonohmic conduction.

From the survey of literature it can be seen that almost no attempt has been made to determine the density of states effective mass m^* from the electrical properties and the *I–V* characteristics in the vicinity of room temperature of the mixed crystals in the $SnSe–Bi_2Se_3$ (corresponding to the stoichiometry $SnBi_4Se_7$) system. Hence, in the present work this art has been suggested for studying. Therefore, it was thought that it would be very interesting to investigate the electrical transport properties of this system over the entire range of temperature.

Experimental procedure

The binary tin and bismuth selenides (SnSe and Bi_2Se_3) were prepared by a solid-state reaction from 5 N purity elements, while the ternary compound $SnBi_4Se_7$ was prepared from the binary compounds. The X-ray investigation and other experimental details about the sample preparation are reported elsewhere [2].

The $SnBi_4Se_7$ compound ingot was cut into two parts. One was left as an as-quenched sample and the other was annealed, which was heated in an evacuated furnace at 573 K for 60 min. This temperature was selected to be above the crystallization temperature (553 K), as calculated from the thermal analysis data (DSC).

Bulk samples (the conduction cross-section ~ 0.5 cm^2 and the length ~ 0.3 cm) with parallel and optically flat

S. A. Ahmed · S. H. Mohamed
Department of Physics, Faculty of Science, Sohag University, Sohag 82524, Egypt

S. A. Ahmed (✉)
Girls College of Education, P.O. Box 3137, Unaizah, Qassim 51911, Kingdom of Saudi Arabia
e-mail: saadzf2003@yahoo.com

surfaces were prepared by a wire saw with a 600-mesh silicon carbide slurry. The best crack-free samples were most easily obtained with an acid saw. For cutting samples, a solution of one part HCL, three parts HNO_3 solution was found satisfactory. Polishing was performed mechanically by means of a controlled velocity rotating disk. A technique developed by Sagar and Faust [12] was used to etch the samples in a dilute solution of bromine (10 mL of a stock solution of 10% bromine in methanol) in methanol (150 mL of methanol), the etching time usually was anywhere from 30 s to 2 min, and then the samples were washed many times in methanol and finally in deionizer water.

The measurements of the current–voltage (*I*–*V*) characteristics and dc electrical conductivity (σ) of as-quenched Bi_2Se_3 and $SnBi_4Se_7$, and annealed $SnBi_4Se_7$ were carried out under vacuum of 10^{-4} mbar, using a pressure contact sample holder. To achieve ohmic contact with the investigated samples a silver paste was used. The achievement of an ohmic contact with the samples is a mandatory condition for investigation of their electrical properties, especially for the $\sigma = f(T)$ dependence. The non-rectifying character of the metal–semiconductor contacts was proved on the basis of the measured current–voltage characteristics. A conventional series electrical current circuit was used. The current was measured directly by means of Gould advance Beta DMM, while the potential difference was measured by means of Keithely 179 μV DMM. The sensitivity of measuring current and potential difference was equal to 1×10^{-6} A and 1×10^{-5} V, respectively. The applied voltage was stepwise swept from zero to the desired value and, in order to reach a steady state, a delay time of 10 up to 30 s was used setting the voltage step and the current reading.

For the purpose of determining the barrier heights of contacts, *I*–*V* measurements were performed at four temperature values, $T = 280$, 300, 320, and 340 K, whereas, the dc conductivity measurements were carried out in the temperature range 90–420 K. The temperature was controlled by means of a thermocouple.

Results and discussion

In a better understanding of electrical properties of any semiconductor material, it has great importance to be known for its contact behavior with several other substances. For this purpose, common analysis methods include current–voltage (*I*–*V*), capacitance–voltage (*C*–*V*), and photoelectric measurements [13–15].

I–*V* characteristics obtained at four temperature values for annealed $SnBi_4Se_7$ is shown in Fig. 1 (for example). Similar plots (results not shown) have been obtained for

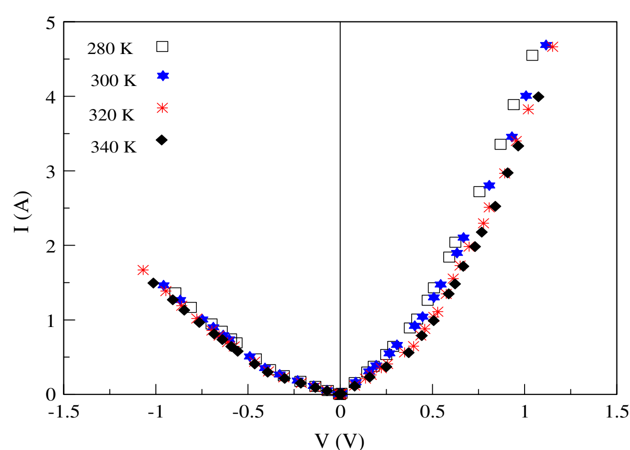

Fig. 1 *I*–*V* characteristics of annealed $SnBi_4Se_7$ under different temperature values

as-quenched Bi_2Se_3 and $SnBi_4Se_7$ under the same conditions. All measurements were performed in a voltage range of ~ -1 V to ~ 1 V. It is found that these curves obey $I \propto V^m$ equation. The value of m is 1 at lower fields (<1.67 V/cm), suggesting ohmic conduction and is between 1 and 2 at higher fields (>1.67 V/cm). Since proportion of defects and nonstoichiometry may not be that high in samples studied it does not influence ohmic conduction in low field region. The behavior at higher fields ($1 \leq m \leq 2$) demonstrates the possibility of space charge limited conduction. Therefore, the *I*–*V* characteristics in the forward direction with $V > 3k_BT/q$ is given by [16];

$$J = A^{**}T^2 \exp(-q\phi_{B0}/k_BT) \exp(qV/nk_BT) \quad (1)$$

where A^{**} is the effective Richardson constant, T the absolute temperature, q the electronic charge, $\phi_{B0}$the barrier height at zero bias, k_B the Boltzmann constant and n the ideality factor.

For each temperature value, ideality factor, n, was calculated by means of the logarithmic *I*–*V* graphs for all samples and given in Table 1. These values have been found to be not in any apparent relation with temperature, except for annealed $SnBi_4Se_7$ sample it decreases with increasing temperature. At all considered temperatures, the values of ideality factor for as-quenched $SnBi_4Se_7$ were found to be greater than those for as-quenched Bi_2Se_3, while the values for annealed $SnBi_4Se_7$ were found to be greater than those for as-quenched $SnBi_4Se_7$.

From the reverse-bias logarithmic I_R–V graphs, saturation current densities were determined for all samples and listed in Table 1. The saturation current values were found to be greater for as-quenched $SnBi_4Se_7$ than those for annealed $SnBi_4Se_7$, while the values for annealed $SnBi_4Se_7$ were greater than those for as-quenched Bi_2Se_3. Furthermore, the saturation current densities have been increased with the temperature for all samples. Also, from the

Table 1 Saturation current densities, ideality factors, carrier concentrations, and barrier heights for contacts at different temperatures of as-quenched Bi_2Se_3 and $SnBi_4Se_7$, and annealed $SnBi_4Se_7$ samples

Sample	Temperature	J_0 (A/m^2)	n	N_D (10^{19} cm^{-3})	ϕ_{B0} (eV)
As-quenched Bi_2Se_3	280	2.406	1.66	4.2	0.320
	300	2.362	1.57	5.5	0.347
	320	2.321	1.63	8.4	0.374
	340	2.236	1.60	11	0.402
As-quenched $SnBi_4Se_7$	280	2.947	1.87	1.7	0.349
	300	2.835	1.77	2.2	0.379
	320	2.748	1.77	3.6	0.409
	340	2.626	1.63	5.1	0.442
Annealed $SnBi_4Se_7$	280	2.664	2.16	2.1	0.335
	300	2.596	2.08	3.4	0.364
	320	2.467	2.00	4.2	0.393
	340	2.378	1.88	6.1	0.423

variation of $\ln(I_s/T^2)$ with (1000/T), effective Richardson parameters, A^{**}, were determined for as-quenched Bi_2Se_3 and $SnBi_4Se_7$, and annealed $SnBi_4Se_7$ as $A^{**} = 8.93$, 22.65 and 13.53 A/cm^2 K^2, respectively. By using these values for Richardson constants and also Eq. 1 at four temperature values, the barrier heights were calculated for all samples, and given in Table 1. An increase for barriers heights with the temperature for all samples was observed.

Furthermore, the apparent built-in potential, V_{bi}, for any contact can be determined by means of the variation of $Ln(I)$ with the inverse temperature, $1/T$. Therefore, an effective potential, $V_{eff} = V + V_{bi}$ can be introduced and the reverse-bias current density might be written as [16];

$$I_R = I_0 \exp\left[\alpha (V_{eff})^{1/4}\right] \tag{2}$$

Here, α is defined as follows:

$$\alpha = \frac{q}{k_B T}\left(\frac{q}{4\pi\varepsilon_s}\right)^{1/2}\left(\frac{2qN_D}{\varepsilon_s}\right)^{1/4} \tag{3}$$

where ε_s is the dielectric constant of semiconductor material and N_D the donor concentration in n-type semiconductor.

Thus, the α parameter in the above equation, and hence N_D carrier densities can be estimated by plotting the $\ln(I_R) - V_{eff}^{1/4}$ graph for each temperature value. Therefore, for as-quenched Bi_2Se_3 and $SnBi_4Se_7$, and annealed $SnBi_4Se_7$ samples, the $\ln(I_R) - V_{eff}^{1/4}$ graphs were plotted in Figs. 2, 3, and 4, respectively. Then, the α parameters found by slopes of curves for each temperature were shown in relevant figures. Taking into account the temperature-independent component of the electrical conductivity, the dielectric constants for all samples are calculated as reported in Ref. [17]. The calculated values for the dielectric constants of as-quenched Bi_2Se_3 and $SnBi_4Se_7$, and annealed $SnBi_4Se_7$ were 30, 26.4, and 26.69, respectively. Using Eq. 3, the values of N_D concentrations were

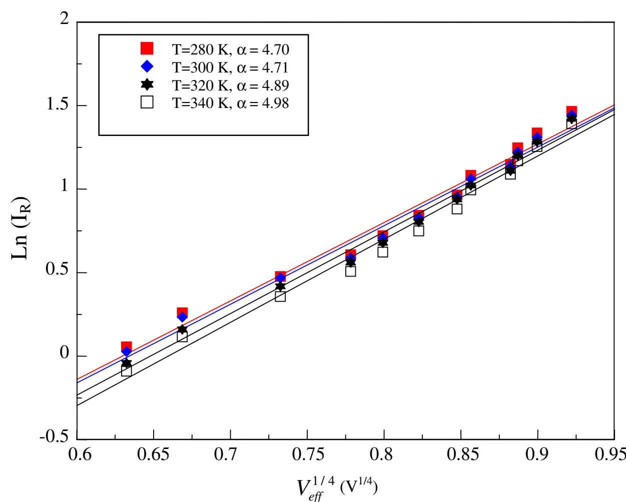

Fig. 2 The variation of reverse current $\ln(I_R)$ with $V_{eff}^{1/4}$ for as-quenched Bi_2Se_3. By means of slopes of these curves, α parameter were determined

obtained and listed in Table 1 for all samples. The carrier density values were found in agreement with those given in literature survey and comparable with those reported below.

Figure 5 shows the electrical conductivity of as-quenched Bi_2Se_3 and $SnBi_4Se_7$, and annealed $SnBi_4Se_7$ samples as a function of temperature. The electrical conductivity measurements on polycrystalline of as-quenched Bi_2Se_3 showed that the material is a semiconductor with conductivity of $\sim$4.81 Ω^{-1} cm^{-1} at 420 K which decreases to $\sim$3.66 Ω^{-1} cm^{-1} at 90 K. While, the electrical conductivity of as-quenched $SnBi_4Se_7$ and annealed $SnBi_4Se_7$ were $\sim$2.51 and 2.92 Ω^{-1} cm^{-1} at 90 K, respectively. Hence, showed a metal-like trend decreasing with elevating temperature [3, 18–20]. However, it reaches a minimum at 200 [3, 18, 19] and 290 K [20], respectively, and

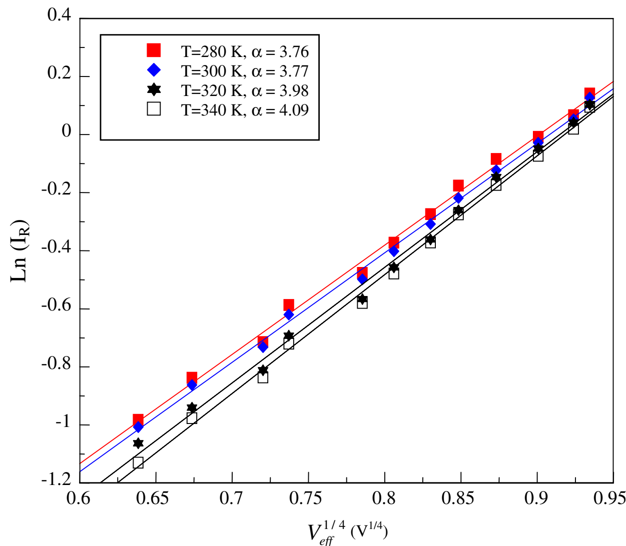

Fig. 3 The variation of reverse current $\ln(I_R)$ with $V_{eff}^{1/4}$ for as-quenched $SnBi_4Se_7$. By means of slopes of these curves, α parameter were determined

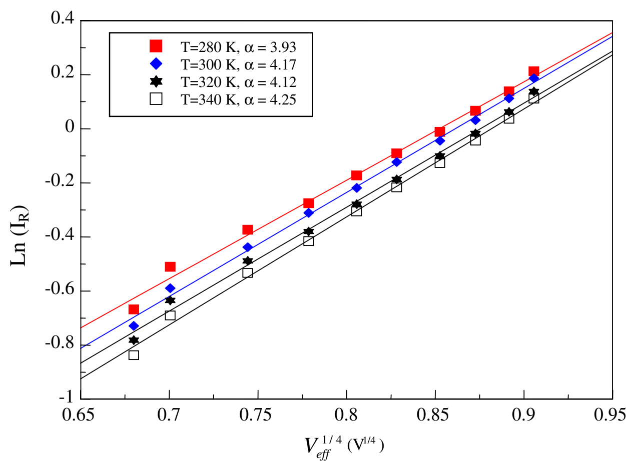

Fig. 4 The variation of reverse current $\ln(I_R)$ with $V_{eff}^{1/4}$ for annealed $SnBi_4Se_7$. By means of slopes of these curves, α parameter were determined

subsequently increases. The low values of the electrical conductivity with the weak temperature dependence between 90 and 420 K suggests that these compounds are semi-metal or narrow-bandgap semiconductor and are in a relatively high doping state (degenerate) as prepared. The electrical conductivity value of the annealed SnBi4Se7 sample is high, except at high temperature, compared with that value of the as-quenched sample, as expected. Since annealing has the effect of altering the nature and concentration of defects, as well as promoting grain growth, and thus material homogeneity. At high temperature the trend could indicate a correlation between grain size and high temperature performance.

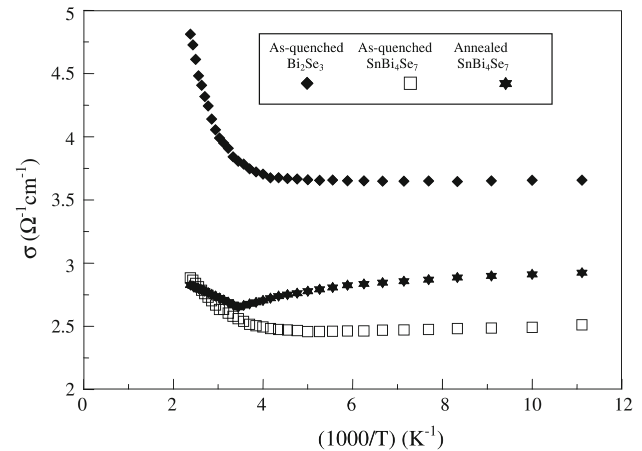

Fig. 5 Electrical conductivity (Ω^{-1} cm^{-1}) versus $1000/T$ characteristics of as-quenched Bi_2Se_3 and $SnBi_4Se_7$, and annealed $SnBi_4Se_7$ samples

Accordingly [3, 18–20], the metal-like behavior of the charge-transport properties of as-quenched $SnBi_4Se_7$ is, therefore, due to heavy doping occurring during synthesis to the point where these materials can be classified as degenerate semiconductors. Such doping could be brought via slight nonstoichiometry between Sn/Bi, slight Se deficiency or slight Se excess [18]. The negative thermoelectric power of the materials [2] indicates electrons as the carriers and is consistent with slight Se deficiency [18].

In order to gain further information regarding the effect of doping with foreign impurities and annealing process on the shallow donor activation energy, the expression proposed by Blakemore for nondegenerate statistics of the single level, applicable to conduction band electrons which are predominant at higher temperatures, is used [21, 22]. This is expressed as [23]:

$$\frac{n_c(n_c + N_A)}{N_D - N_A - n_c} = \frac{N_C}{2}\exp\left[\frac{-E_D}{k_B T}\right], \tag{4}$$

where

$$N_C = \frac{2}{h^3}\left[2\pi m_e^* k_B\right]T^{3/2} \tag{5}$$

In these expressions E_D is the activation energy and m_e^* the effective mass of electrons, n_c the electron concentration in the conduction band, N_D and N_A are the concentration of donors and compensating acceptors, respectively and $k = N_A/N_D$ the compensation ratio. The carrier density n_c was calculated, as that reported in many articles [24–28]. To calculate the values of N_D, N_A, and E_D a method, originally proposed by Huston [29] and later successfully employed by Marin et al. [21] and Wasim et al. [22], is used. Following this approach trial values of N_D and N_A are chosen and with the temperature

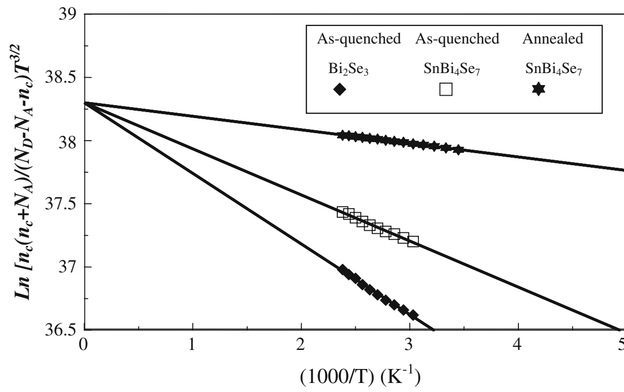

Fig. 6 A plot of $\ln\left[n_c(n_c+N_A)/(N_D-N_A-n_c)T^{3/2}\right]$ against 1000/*T* for as-quenched Bi_2Se_3 and $SnBi_4Se_7$, and annealed $SnBi_4Se_7$ samples

dependence of the calculated n_c, $\ln[n_c(n_c+N_A)/(N_D-N_A-n_c)T^{3/2}]$ is plotted against 1000/*T*. If the plot does not give a straight line, new values of N_D and N_A must be chosen and the calculated data are replotted. This process is repeated until a straight line over a temperature range up to 300 K, where the conduction in the activation regime is predominant, is obtained for all samples. This gives the correct value of N_D and N_A. This is shown in Fig. 6, and the values of N_D and N_A are given in Table 2. From the slope of the linear dependence, thus obtained in Fig. 6, E_D is calculated for all samples. Values of E_D estimated from the slope for as-quenched Bi_2Se_3 and $SnBi_4Se_7$, and annealed $SnBi_4Se_7$ samples are also given in Table 2. It can be noticed that the straight lines converge, within the experimental error, to a single point at *y*-axis ($1000/T = 0$). Since the effective mass m_e^* is calculated from the intercept at *y*-axis, the convergence confirms that m_e^* does not change for all samples. This type of analysis of the electrical conductivity dependence of temperature, to our knowledge, has not been reported before. This helps us to determine the effective mass, with greater accuracy. The electron effective mass m_e^* of as-quenched Bi_2Se_3 and $SnBi_4Se_7$, and annealed $SnBi_4Se_7$ samples, estimated from the intercept, is given in Table 2. Kuznetsova et al. [20] reported that the calculated density of state effective masses for the ternary Ge(Sn,Pb)Te–Bi_2Te_3 compounds have similar values to those for Bi_2Te_3. Accordingly [30], the density of state effective masses for the ternary compounds of Bi_2Se_3 doped with different foreign elements (Pb–Bi_2Se_3, for example [30]) have similar values to those for Bi_2Se_3. From our study we obtained an average of $m_e^* = 0.15 \pm 0.001$, related to the free electron mass m_0, in excellent agreement with that reported in Refs. [10, 31].

From the slope of the linear fits in Fig. 6, the activation energy E_D for all samples is calculated. This is given in Table 2. As seen from Table 2, the value of E_D decreases from $E_D = 48.1$ meV to $E_D = 9.2$ meV as the compensation is raised from $N_A/N_D = 0.15$ to $N_A/N_D = 0.24$. Similar behavior was reported in Ref. [32], and as the ionized impurity is increased as well (to be published elsewhere). Castellan and Seitz [33] suggested that the decrease of activation energy with concentration was due to the potential energy of attraction between the ionized donors and conduction electrons. They considered that, this mechanism would lead to lower the activation energy which is inversely proportional to the average distance between an electron and an ion. Another source of lowering of the activation energy lies in polarization effects. The substitution of Sn atoms for Bi in the Bi_2Se_3 lattice causes an increase in the polarization of the studied samples [34], and lowers the edge of the conduction band and consequently the activation energy [35]. However, because of the limited number of data points, no conclusive information about E_D in the dilute limit can be obtained from the E_D versus $N_D^{1/3}$ plot [36].

Conclusions

In summary, we have investigated the transport properties of polycrystalline samples of Bi_2Se_3 and stoichiometric ternary compound in the quasi-binary system SnSe–Bi_2Se_3. The current–voltage (*I*–*V*) characteristics measurements show Richardson–Schottky emission in high field region. Since proportion of defects and nonstoichiometry may not be that high in samples studied it does not influence ohmic conduction in low field region.

On the other side, the effect of doping with foreign impurities and annealing process in the activation regime above 300 K is studied. The analysis of the temperature dependence of electron concentration, using Blakemore

Table 2 Donor and acceptor concentration, compensation ratio, electron effective mass, and ionization energies of as-quenched Bi_2Se_3 and $SnBi_4Se_7$, and annealed $SnBi_4Se_7$ samples

Sample	N_A (10^{19} cm^{-3})	N_D (10^{19} cm^{-3})	K	m_e^* (m_0)	E_D (meV)
As-quenched Bi_2Se_3	0.71	4.80	0.15	0.149	48.1
As-quenched $SnBi_4Se_7$	0.65	2.73	0.24	0.151	30.9
Annealed $SnBi_4Se_7$	0.61	2.52	0.24	0.149	9.2

model, permits to estimate the effective mass of the majority charge carrier with greater accuracy for all samples. The value of $m_e^* = (0.15 \pm 0.001)m_0$ has an excellent agreement with those reported earlier.

Acknowledgements One of the authors (S. A. Ahmed) would like to thank Professor M. M. Wakkad for critical revising of the manuscript. He is also grateful to Dr. M. R. Ahmed and Dr. S. S. Sheishaa for their helpful English language support.

References

1. Birkholz U (1984) In: Heywang W (ed) Amorphe und Polykristalline Halbleiter, Berlin
2. Ahmed SA (2006) Philos Mag 86(9):1227
3. Ahmed SA, Ibrahim EMM, Saleh SA (2006) Appl Phys A 85:177
4. Choi J, Lee H-W, Kim B-S et al (2006) J Magn Magn Mater 304:e164
5. Urazhdin S, Bile D, Mahanti SD et al (2004) Phys Rev B 69: 85313
6. Al Bayaz A, Giani A, Foucaran A et al (2003) Thin Solid Films 441:1
7. George SD, Augustine S, Mathai E et al (2003) Phys Stat Sol A 196(2):384
8. Greanya VA, Tonjes WC, Liu R et al (2002) J Appl Phys 92(11):6658
9. Urazhdin S, Bile D, Tessmer SH et al (2002) Phys Rev B 66: 161306
10. Navratil J, Plechacek T, Horak J et al (2001) J Solid State Chem 160:474
11. Nikam PS, Aher HS (1996) Indian J Pure Appl Phys 34:393
12. Sagar A, Faust JW (1967) J Appl Phys 38:482
13. Morsli M, Amory C, Bougrine A et al (2007) J Phys D: Appl Phys 40:7675
14. Mikhelashvili V, Eisenstein G, Uzdin R (2001) Solid-State Electron 45:143
15. Sharma DK, Narasimhan KL, Kumar S et al (1989) J Appl Phys 65(5):1996
16. Sze SM (1981) Physics of semiconductor devices, 2nd edn. Wiley & Sons, New York
17. Simon R (1962) J Appl Phys 33:1830
18. Chung D-Y, Choi K-S, Iordanidis L et al (1997) Chem Mater 9:3060
19. Cho S, DiVenere A, Wong GK et al (1999) Phys Rev B 59:10691
20. Kuznetsova LA, Kuznetsov VL, Rowe DM (2000) J Phys Chem Solids 61:1269
21. Marin G, Wasim SM, Sanchez Perez G et al (1998) J Electron Mater 27:1351
22. Wasim SM, Essaleh L, Rincon C et al (2005) J Phys Chem Solids 66:1887
23. Blakemore JS (1962) Semiconductors Statistics. Pergamon Press, USA
24. Nalos GS, Cohn JL, Dyck JS et al (2002) Phys Rev B 65:165201
25. Dyck JS, Chen W, Yang J et al (2002) Phys Rev B 65:115204
26. Khan ZH, Zulfeqaur M, Kumar A et al (2002) Can J Phys 80:19
27. Pujari VB, Gaikwad VB, Masumdar EU et al (2002) Turk J Phys 26:407
28. Osinniy V, Jedrzejczak A, Arciszewska M et al (2001) Acta Physiol Pol A 100:327
29. Huston AR (1959) J Phys Chem Solids 8:467
30. Karamazov S, Horak J, Navratil J et al (1997) Cryst Res Technol 32(2):249
31. Horak J, Vlcek M, Navratil J et al (1999) Sci Pap Univ Pardubice, Czech Republic
32. Essaleh L, Wasim SM, Galibert J (2001) J Appl Phys 90:3993
33. Castellan GW, Seitz F (1951) Semiconducting materials. Butterworths Scientific Publications, London
34. Perez Vicente C, Tirado JL, Adouby K et al (1999) Inorg Chem 38:2131
35. Debye PP, Conwell EM (1954) Phys Rev 93:693
36. Wasim SM, Albornoz JG (1988) Phys Stat Sol A 110(2):575